

Silica encapsulated ZnO quantum dot-phosphor nanocomposites: Sol-gel preparation and white light-emitting device application

Ya-Chuan Liang(梁亚川), Kai-Kai Liu(刘凯凯), Ying-Jie Lu(卢英杰), Qi Zhao(赵琪), Chong-Xin Shan(单崇新)

Citation: Chin. Phys. B . 2018, 27(7): 078102. **doi:** 10.1088/1674-1056/27/7/078102

Journal homepage: http://cpb.iphy.ac.cn; http://iopscience.iop.org/cpb

What follows is a list of articles you may be interested in

Anomalous temperature dependence of photoluminescence spectra from InAs/GaAs quantum dots grown by formation-dissolution-regrowth method

Guan-Qing Yang(杨冠卿), Shi-Zhu Zhang(张世著), Bo Xu(徐波), Yong-Hai Chen(陈涌海), Zhan-Guo Wang(王占国)

Chin. Phys. B . 2017, 26(6): 068103. **doi:** 10.1088/1674-1056/26/6/068103

Enhanced biocompatibility of ZnS:Mn quantum dots encapsulated with *Aloe vera* extract for therapeutic applications

Anilkumar M, Bindu K R, Sneha Saj A, Anila E I

Chin. Phys. B . 2016, 25(8): 088103. **doi:** 10.1088/1674-1056/25/8/088103

Wavelength-tunable prism-coupled external cavity passively mode-locked quantum-dot laser

Wu Yan-Hua, Wu Jian, Jin Peng, Wang Fei-Fei, Hu Fa-Jie, Wei Heng, Wang Zhan-Guo

Chin. Phys. B . 2015, 24(6): 068103. **doi:** 10.1088/1674-1056/24/6/068103

Density behaviors of Ge nanodots self-assembled by ion beam sputtering deposition

Xiong Fei, Yang Tao, Song Zhao-Ning, Yang Pei-Zhi

Chin. Phys. B . 2013, 22(5): 058104. **doi:** 10.1088/1674-1056/22/5/058104

Tuning nano-pillar array for enhancing the photoluminescence extraction efficiency of GaN-based light-emitting diodes

Chen Xia, Liang Zhu-Hong, Chen Zhan-Xu, Yang Wei-Ming, Chen Tu-Fu, Jin Chong-Jun, Zhang Bai-Jun

Chin. Phys. B . 2013, 22(4): 048101. **doi:** 10.1088/1674-1056/22/4/048101

Silica encapsulated ZnO quantum dot-phosphor nanocomposites: Sol-gel preparation and white light-emitting device application*

Ya-Chuan Liang(梁亚川)[1], Kai-Kai Liu(刘凯凯)[2,†], Ying-Jie Lu(卢英杰),[1]
Qi Zhao(赵琪)[1], and Chong-Xin Shan(单崇新)[1]

[1] School of Physics and Engineering, Zhengzhou University, Zhengzhou 450001, China
[2] State Key Laboratory of Luminescence and Applications, Changchun Institute of Optics, Fine Mechanics and Physics, Chinese Academy of Sciences, Changchun 130033, China

(Received 29 April 2018; revised manuscript received 6 May 2018; published online 25 June 2018)

ZnO quantum dots (QDs) as an eco-friendly and low-cost material has bright fluorescence, which makes it promising material for healthy lighting and displaying. However, the low fluorescence efficiency and poor stability of ZnO QDs impede their applications in lighting application. In this work, silica encapsulated ZnO QD-phosphors nanocomposites (ZSPN) have been prepared through a sol-gel synthesis process, where yellow-emitting ZnO QDs and blue-emitting $BaMgAl_{10}O_{17}:Eu^{2+}$ are employed as the luminescence cores and silica as link between two luminescence materials. Tunable photoluminescence of ZSPN and the white light emission have been achieved through changing mass ratio of both of ZnO QDs and commercial phosphors. The PLQY of the ZSPN can reach 63.7% and they can maintain high luminous intensity even the ambient temperature up to 110 °C and after 35 h of UV irradiation. In addition, they can keep stable for 40 days. By coating the ZSPN phosphors onto a ultraviolet chip, WLEDs with luminous efficiency of 73.6 lm/W and the color coordinate, correlated color temperature, and color rendering index can reach (0.32, 0.34), 5580 K, and 87, respectively, indicating the bright prospect of the ZSPN phosphors used in healthy lighting.

Keywords: ZnO QD-phosphors nanocomposites (ZSPN), phosphors, light-emitting diodes

PACS: 81.07.Ta, 81.16.Be, 81.20.Fw **DOI:** 10.1088/1674-1056/27/7/078102

1. Introduction

White light-emitting diodes (WLEDs) have been considered as promising lighting devices due to their unique merits such as high luminous efficiency, low energy consumption, and long operational life, etc.[1–7] Currently, the main way to achieve WLEDs are to coat yellow-light-emitting phosphors on the InGaN blue chip and the phosphors emit yellow light under blue light excitation, and white luminescence can be obtained when yellow and blue light are mixed.[8,9] In this process, the blue light emitted from the InGaN blue chip participates in the mixing of white light and the performance of the WLED will be affected by the aging of the chip. The above problem drives people to develop UV-pumped WLEDs.[10,11] No matter in fabricating UV-pumped or blue light-pumped WLEDs, phosphors as down-conversion layer play a key role in determining the performance of WLEDs.[2,3,12–15] Nowadays, so far the common used phosphors for commercial WLEDs are rare-earth based luminescence materials.[16–20] However, the reservation of rare-earth element in the world is declining year by year and this tremendously increases manufacturing costs of rare-earth phosphors. Quantum dot may be a possible alternative to rare earth based phosphors. Recently, quantum dot LEDs (QD-LEDs) have drawn much attention due to their tunable emission wavelengths, narrow emission, high luminous efficiency, etc.[21–27] But high-performance QDs usually involve Cd ions, which will endanger human health. Hence, it is of crucial importance to develop eco-friendly and low-cost phosphors replace or reduce the use of rare-earth base and Cd-base quantum dot phosphors.

Zinc oxide (ZnO), one of the most promising semiconductor materials, have been investigated extensively due to their unique properties such as environmentally friendly, simple preparation, low cost, and they will show bright luminescence when it is tailored into nanoscale size. Thanks to the above advantages, ZnO has been applied in bioimaging,[28,29] encryption,[30] photoelectric devices,[31–33] etc. In our previous work, we have coated the ZnO QD phosphors onto ultraviolet (UV) chips and successfully fabricated yellow LEDs which indicates that ZnO QDs have great potential in UV-pumped WLEDs.[34] However, the low quantum yield (QY) of ZnO QDs limits their application in WLEDs. Currently, one of the most effective ways for the development of ZnO QDs in WLEDs is to increase quantum yield. We have developed a way to fabricate ZnO QDs with QYs of 42%, which is the highest value to the best our knowledge. But this is still not enough to apply ZnO QDs as a down-conversion layer in WLED. Compared with ZnO QDs, commercial phosphors have a excellent merit of high quantum yield, which is ad-

*Project supported by the National Natural Science Foundation of China (Grant Nos. 21601159, 61604132, and U1604263) and the National Science Fund for Distinguished Young Scholars of China (Grant No. 61425021).

†Corresponding author. E-mail: 1102570572@qq.com

© 2018 Chinese Physical Society and IOP Publishing Ltd

equate for the commercialization of WLEDs. However, its high cost and complex preparation process hinder their application in LEDs. Moreover, it is a suitable way that combining eco-friendly yellow-emitting ZnO QDs with those commercial blue-emitting phosphors to increase the quantum yield of ZnO QDs and decrease cost of phosphors at the same time.

In this work, multi-emitting ZnO-Silica-Phosphors core–shell nanocomposite (ZSPN) has been designed and fabricated to achieve white light emission for the first time through a one-step sol-gel synthesis process. In this structure, ZnO QDs and phosphors act as luminescence cores and silica acts as link between two luminescence materials. The solid-state ZSPN powders exhibit quite high quantum efficiency (QY = 63.7%) with dual color emission (450 nm and 550 nm) and both of ZnO QDs and phosphors have a strong absorption in UV area which reveal that ZnO QDs and phosphors can be excited simultaneously when they are coated together. Benefiting from the above merits of the structure, tunable emission has been achieved from the ZSPN powders by changing the mass ratio of the ZnO QDs and phosphors. The white light-emitting diodes (WLEDs) have been achieved by coating ZSPN in 365 nm line of a UV chip. The correlated color temperature (CCT), Commission International de L'Eclairage (CIE) coordinate, luminous efficiency and color rendering index (CRI) is 5610 K, (0.32, 0.34), 73.6 lm/W and 87, which indicate the potential applications of ZSPN in eco-friendly and high-efficient LEDs.

2. Methods

2.1. Materials

The precursors used in this study include zinc acetate dihydrate ($Zn(Ac)_2{\cdot}2H_2O$, purity > 99%), potassium hydroxide (KOH, purity > 99%), 3-aminopropyltriethoxysilane (APTES, purity > 98%), $BaMgAl_{10}O_{17}:Eu^{2+}$ phosphors, tetraethoxysilane (purity > 99.9%), ethanol (purity > 99.9%), etc. All of the chemicals were purchased from Macklin Chemistry Co. Ltd (Shanghai, China). Note that all the chemicals used in this work were analytical grade without further purification.

2.2. Synthesis of ZnO QDs

The ZnO QDs were prepared according to the method reported in our previous work.[34] 5.5 g (25 mmol) $Zn(Ac)_2{\cdot}2H_2O$ was dissolved in 150 mL ethanol solution and the solution was refluxed under continuous stirring for 30 min at room temperature. Then 20 mL 35 mmol KOH solution was added into the $Zn(Ac)_2{\cdot}2H_2O$ ethanol solution under continuous stirring for 10 min. Then mixtures of 1.5 mL deionized water and 400 μL 3-aminopropyltriethoxysilane (APTES) were added into the above solution under continuous stirring for 2 h. After that, the obtained precipitates were washed using ethanol for three times to remove the unreacted precursors. Finally, the ZnO QDs precipitates were dried in an oven at 70 °C for 6 h to form ZnO QD powders.

2.3. Synthesis of ZSPN

The ZnO QDs (150 mg (1), 140 mg (2), 130 mg (3), 120 mg (4)) tetraethoxysilane (TEOS, 1 mL) were dispersed in water to form a aqueous solution. Then, $BaMgAl_{10}O_{17}:Eu^{2+}$ powder (15 mg) was placed into the above solution stirring at room temperature for 8 h. The precipitates were washed using water for three times to remove the unreacted precursors. Finally, the ZSPN nanocomposite was dried in an oven at 70 °C for 8 h to form ZSPN powders.

2.4. Fabrication of LEDs

For the fabrication of WLED, epoxy resin was premixed with the ZSPN phosphors. The mixture was packaged onto the UV chip with 365 nm. After that, the as-prepared LED were placed into an oven at 80 °C for 2 h to fabricate WLEDs.

2.5. Characterizations

X-ray diffraction (XRD) patterns were obtained on X'Pert Pro diffractometer. TEM (JEM-2010) was employed to characterize the size and crystallinity of the samples. Fluorescence spectra and PLQYs were obtained on Hitachi F-7000 spectrophotometer. The luminous efficiency is recorded by radiometers PM6612L. UV–vis absorption spectra were obtained using a UH4150 spectrophotometer.

3. Results and discussion

The yellow-emitting ZnO QDs, blue-emitting phosphors, and TEOS were selected as members of ZSPN and the ZSPN was prepared by one-step sol-gel synthesis process. The ZnO QDs using in this paper were prepared according to the method reported in our previous work.[34] The size of ZnO QDs will determine the emission color and there have been many references discussing this color dependence.[29] In this work, the size of as-prepared ZnO QDs is about 5 nm and they can emit bright yellow fluorescence when they are exposed under UV radiation (Fig. S1, Supporting Information). ZnO QDs have been functionalized with (3-aminopropyl) triethoxysilane (APTES) and there are abundant silanol groups (Si–OH) in their surface. The corresponding FTIR spectrum has been indicated in Fig. S2. The blue-emitter used in this paper is $BaMgAl_{10}O_{17}:Eu^{2+}$ and they have the merits of high luminous efficiency, superior thermal and photo stability. The formation process of the ZSPN was illustrated in Fig. 1. The ZnO QDs solution will be alkaline due to the existence of amino (Fig. S2, Supporting Information), so the formation process of the ZSPN is a selfhydrolysis process, which makes it simple and eco-friendly for the large-scale synthesis of ZSPN and

pay the way for their future applications. Under hydrolysis of TEOS in the ZnO QDs and phosphors solution, ZnO QDs will covalently bind to silica by forming Si–O–Si bonds and there form a silicon layer alternating with ZnO QDs will be coated on the phosphor due to a polymerization process. Finally, a multi-emitting core–shell structure will be formed.

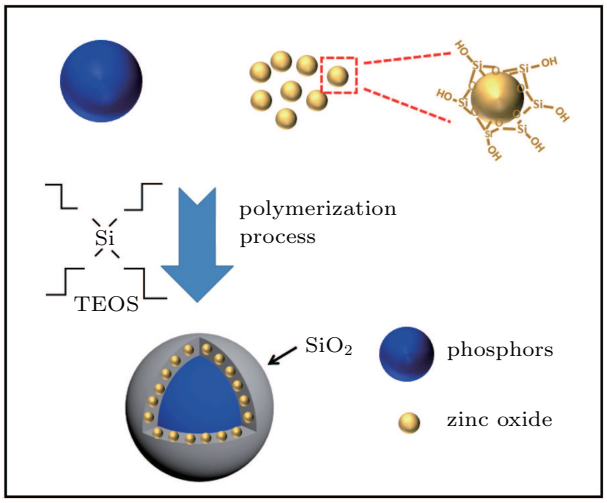


Fig. 1. (color online) Schematic illustration of the formation process of the ZSPN.

The morphology of the ZSPN has been characterized by transmission electron microscope (TEM). From the TEM image shown in Fig. 2(a), spherical-like microstructures can be observed clearly from the image and the particle sizes is about 88.9 nm, as shown in Fig. 2(b). There are two phases in ZSPN structure. It can be seen that transparent section is silica cell and dark section is phosphors core. The above data demonstrates that the phosphor is uniformly coated with ZnO–silica cell on the outside after a simple sol-gel process. In order to analyze the elements of the ZSPN, elemental mapping using energy-dispersive x-ray spectroscopy (EDX) was recorded, as shown in Fig. 2(c). The elements of Zn, O, Ba, Mg, Al, Eu, and Si can be observed from the figure. The elements of Zn and O come from ZnO QDs and the elements of Ba, Mg, Al, Eu come from $BaMgAl_{10}O_{17}:Eu^{2+}$. The distribution of Si, Zn, and O element match well with that of the rest of the elements, indicating the ZnO-silica cell has successfully coated phosphor. The XRD patterns of the ZnO QDs, phosphors and ZSPN have been illustrated in Fig. 2(d). The broad peak centered at around 23° come from silica, while all the other peaks correspond well to hexagonal wurtzite ZnO structure and $BaMgAl_{10}O_{17}:Eu^{2+}$. From the XRD pattern of the ZSPN, the peaks corresponding to both ZnO QDs and $BaMgAl_{10}O_{17}:Eu^{2+}$ can be observed simultaneously, which reveal that phosphors have been coated by ZnO silica.

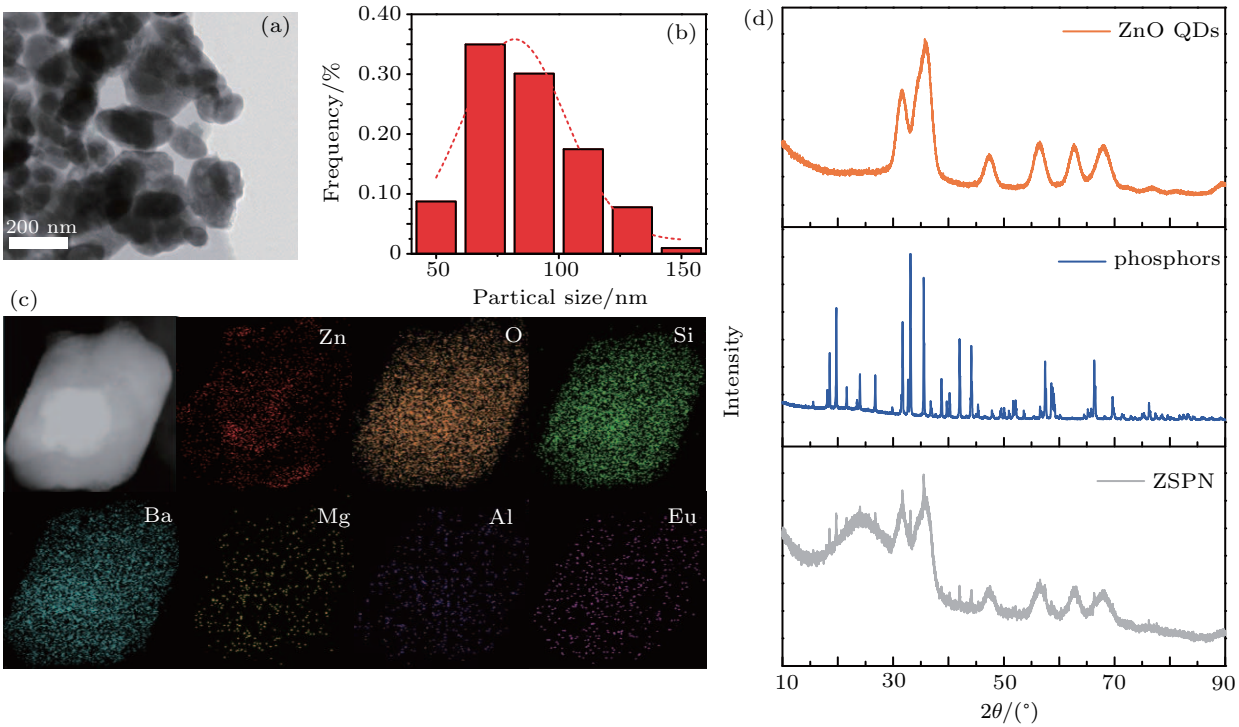


Fig. 2. (color online) (a) TEM image of the ZSPN nanocomposite; (b) the statistical size distribution of the ZSPN nanocomposite; (c) elemental mapping of the ZSPN nanocomposite; (d) XRD pattern of the ZnO QDs, $BaMgAl_{10}O_{17}:Eu^{2+}$, and ZSPN.

Fourier transform infrared (FTIR) spectra of the ZnO QDs, phosphors and ZSPN were recorded, as shown in Fig. 3(a). In the FTIR spectrum of the ZnO QDs, the peaks centered at around 480 cm^{-1}, 1405 cm^{-1}, and 1574 cm^{-1} can be attributed to the stretching vibration of Zn–O, C–H, and N–H respectively. In the FTIR spectrum of the phosphors, the peaks centered at 600–700 cm^{-1} can be attributed to the stretching vibration of Al–O stretching bands. In the

FTIR spectrum of the ZSPN, the peak at 1075 cm^{-1} can be attributed to vibration absorption of SiO_2, which indicates the formation of silica cell. In addition, the Zn–O stretching bands at around 480 cm^{-1} and the Al–O stretching bands at around 600–700 cm^{-1} can be observed in both the ZSPN and ZnO QDs, indicating that the phosphors have been coated by the ZnO-silica cell. In addition, the x-ray photoelectron spectroscopy (XPS) was used to analysis the element of ZSPN, as shown in Fig. 3(b). In Fig. 3(b), the peaks including Zn 2p, Si 2p, Ba 4s, Eu 3d, Mg and O 1s appear simultaneously. The Si 2p at 103.9 eV for Si–O bands indicating the Si–O band has formed and silicon layer alternating with ZnO QDs have been coated on the phosphor.

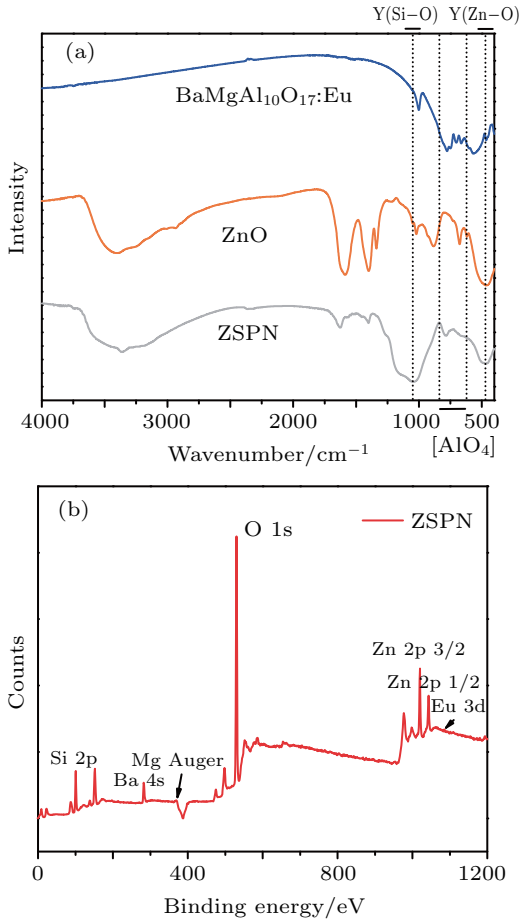


Fig. 3. (color online) (a) FTIR spectra of the nanocomposite; (b) XPS spectra of the nanocomposite.

To study the optical properties of as-prepared ZSPN, the photoluminescence spectra and excitation spectra of both of ZnO QDs and phosphors were measured as shown in Fig. 4(a) and 4(b). Figure 4(a) shows optical properties of ZnO QDs. The emission range of the ZSPN powders is from 430 to 720 nm and the maximum emission peak in 550 nm. The corresponding optimal excitation peak is 365 nm. In addition, the emission peak of ZnO QDs is a broad peak, indicating that ZnO QDs are suitable yellow down-conversion layer for UV-pumped WLEDs. $BaMgAl_{10}O_{17}:Eu^{2+}$ phosphor can be effectively excited at a broad range of wavelengths from 200 to 400 nm and the corresponding emission peak is 450 nm as shown in Fig. 4(b). It is evidenced from the figure that both of the emission peaks at around 550 nm and 450 nm can be observed when the excitation wavelength is 365 nm, indicating the highest brightness emission of ZnO QDs and $BaMgAl_{10}O_{17}:Eu^{2+}$ phosphor can be achieved under UV radiation and the powders can be used as UV-pumped down-conversion layer. SiO_2 precipitate has been obtained by a sol-gel process, and no fluorescence can be observed and the corresponding fluorescence spectra and photographs of SiO_2 are shown in Fig. S3. The spectra of the as-fabricated ZSPN consist of two emission peaks centered at around 450 nm and 550 nm with almost equal intensity, which can be assigned to the emission from the $BaMgAl_{10}O_{17}:Eu^{2+}$ phosphors and ZnO QDs, respectively. Under the excitation of 365 nm line, the PLQY of the ZSPN powders is 63.7%. PLQY is a key factor that determines the performance of phosphors, so the ZSPN may promise their bright prospect in lighting and displaying. The fluorescence images of the ZnO QDs, ZSPN, and $BaMgAl_{10}O_{17}:Eu^{2+}$ phosphor under indoor and UV lighting conditions are shown in Fig. 4(d). The all powders are white in color under the indoor lighting conditions. Under the excitation of the 365 nm line of a UV lamp, ZnO QDs show bright yellow luminescence and $BaMgAl_{10}O_{17}:Eu^{2+}$ phosphor show bright blue luminescence, while the ZSPN show strong white luminescence. The above data confirm further that the $BaMgAl_{10}O_{17}:Eu^{2+}$ phosphors have been coated by ZnO-silica.

The tunable luminescence spectra of the ZSPN and white light emission can be achieved by varying the mass ratios of ZnO QDs and $BaMgAl_{10}O_{17}:Eu^{2+}$ phosphor, and the corresponding photoluminescence (PL) spectra of the ZSPN powders are shown in Fig. 5(a). By controlling the mass ratio of the ZnO QDs and $BaMgAl_{10}O_{17}:Eu^{2+}$ phosphor (10:1(1), 9.3:1(2), 8.7:1(3), 8:1(4)), the yellow emission is decreased obviously. The corresponding color of ZSPN can be tuned from cool white to warm white. The as-prepared tunable luminescence ZSPN phosphors show bright fluorescence under UV illumination, as shown in Fig. 5(d). White emission with the CIE coordinate of (0.32, 0.34) can be realized, which is very close to the standard CIE coordinate of WLED (0.33, 0.33). The corresponding tunable luminescence CIE coordinate were shown in Fig. 5(e). The ability of anti-photobleaching is a key indicator that determines the performance of phosphors used in WLED, so the optical stability of the ZSPN powder were assessed. ZSPN with different mass ratios of ZnO QDs and $BaMgAl_{10}O_{17}:Eu^{2+}$ phosphor (10:1(1), 9.3:1(2), 8.7:1(3), 8:1(4)) were irradiated under a strong UV beam of 365 nm from a fluorescence spectrofluorometer (photomultiplier of 650 V) for 3600 s. The PL intensity of both of 450 nm and

550 nm can maintain more than 90%, as indicated in Figs. 5(b) and 5(c). To further evaluate the longtime photostability, the ZSPN (3) was put under a hand-held UV lamp (0.15 mW/cm^2) for 35 hours. The corresponding luminescence spectra and the dependence of the luminescence intensity of the peaks centered at 450 nm and 550 nm has been shown in Fig. S4 and Fig. 5(f). The photostability of ZnO QDs is less stable than that of $BaMgAl_{10}O_{17}:Eu^{2+}$ phosphor upon continuous ultraviolet radiation. This result seems to be acceptable as it is more stable than other phosphors used in WLEDs. However, the PL intensity of ZSPN can maintain more than 90% after 35 hours of UV illumination as shown in Fig. 5(f). The characteristic of anti-photobleaching in ZSPN ensures their PL stability under long time ultraviolet radiation when packaged it on UV chips.

In order to analyze structural stability of ZSPN, the as-prepared ZSPN has been washed following a centrifugation process for 6 cycles. The corresponding luminescence spectra and the dependence of the fluorescence intensity of the peaks centered at 550 nm of the ZSPN after washing were measured as shown in Figs 6(a) and 6(b). There is no apparent change in PL intensity and lineshape of the ZSPN, indicating there is no phase separation and the good structural stability of the ZSPN. In addition, thermal stability is another important factor for phosphors used in LEDs, thus the thermal stability of the as-prepared sample is analyzed by annealing the ZSPN (3) under different temperature. The dependence of the PL intensity of the peaks centered at 450 nm and 550 nm on annealing temperatures has been shown in Fig. 6(c). The PL intensity of two peaks keeps unchanged even the temperature is increased to 110 °C, the corresponding images of the ZSPN annealed at different temperature are shown in the inset of Fig. 6(c). The line shape and PL intensity of the ZSPN remain almost unchanged while the emission intensity decreases a little when the annealing temperature reaches 110 °C as shown in Fig. S5. The above date indicated that the as-prepared ZSPN can keep high performance when they are operating at high temperatures. Phosphors used in WLED always need to work for a long time, thus temporal stability of phosphors determines the performance of WLEDs. The temporal stability of the ZSPN was measured under ambient conditions, as shown in Fig. 6(d). The line shape and PL intensity of the two peaks remain almost unchanged within 40 days (Fig. S6), indicating the good stability of the ZSPN in ambient conditions.

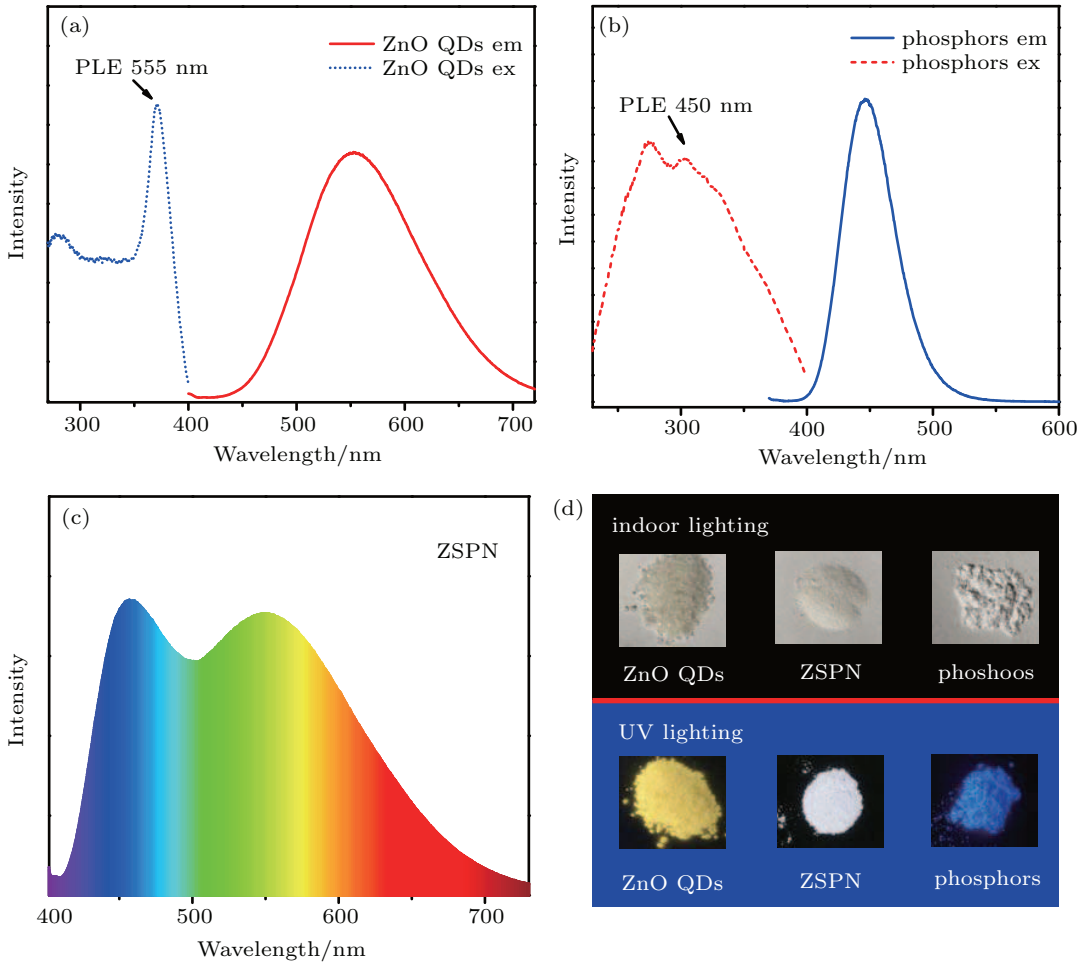


Fig. 4. (color online) (a) Fluorescence excitation (ex) and emission (em) spectra of ZnO QDs; (b) fluorescence excitation (ex) and emission (em) spectra of $BaMgAl_{10}O_{17}:Eu^{2+}$; (c) fluorescence spectra of the ZSPN nanocomposite; (d) images of the ZnO QD, ZSPN, and $BaMgAl_{10}O_{17}:Eu^{2+}$ under indoor lighting and UV lighting conditions.

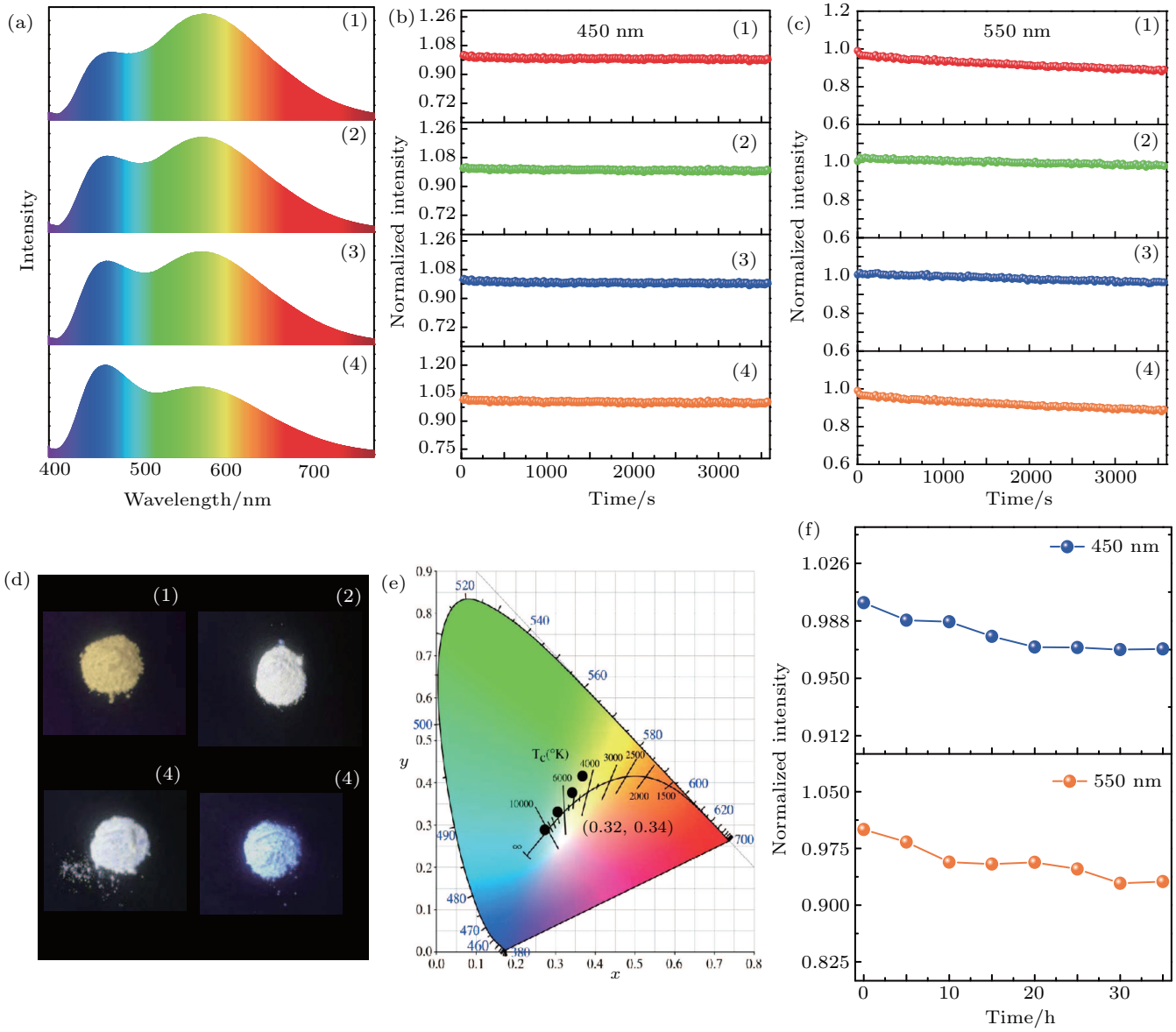


Fig. 5. (color online) (a) Fluorescence emission spectra of ZSPN with different mass ratio of the ZnO QDs and $BaMgAl_{10}O_{17}:Eu^{2+}$; (b) the photostability of the ZSPN under a UV beam of 365 nm from a fluorescence spectrofluorometer by monitoring the emission peaks of the $BaMgAl_{10}O_{17}:Eu^{2+}$ (450 nm); (c) the photostability of the ZSPN under a UV beam of 365 nm from a fluorescence spectrofluorometer by monitoring the emission peaks of the ZnO QDs (550 nm); (d) the corresponding images of the ZSPN; (e) the corresponding CIE coordinates of the ZSPN; (f) the photostability of the ZSPN under hand-held UV lamp of 365 nm.

Based on the above merits, UV-pumped LEDs have been fabricated by mixing ZSPN with epoxy resin, and the mixture were coated onto the chips of 365 nm UV-chips. The electroluminescence (EL) intensity of the WLED increased when the drive current increased from 10 to 100 mA as shown in Fig. 7(a). The corresponding CCT and CIE coordinate shows slight changes from 5580 K to 5618 K, (0.3155, 0.3410) to (0.3275, 0.3464), respectively. The luminous efficiency slightly dropped from 73.6 to 68.5 lm/W. The maximum luminous efficiency is 73.6 lm/W when injection current is 50 mA. The recent reported QDs-based phosphors are summarized in Table 1. The reason for the change of luminous efficiency when the drive current increased from 10 to 100 mA is that the luminous efficiency is closed to the external quantum efficiency of UV chip and the quantum efficiency of UV chip increases first and then decreases with the injection current. As a result, the luminous efficiency of LEDs increases first and then decreases with the injection current from 10 to 100 mA. These results show that the ZSPN phosphors have high stability against the change of driven current. The CRI of the as-prepared WLED is 87, and a chromophotograph was used to assess the color rendering ability of the WLED further, as shown in Fig. 7(d). The picture taken under the irradiation of the as-prepared WLED (50 mA) show the true colors of the picture. Thanks to the co-friendly and abundant properties of ZSPN, the results may apply a bright prospect in healthy lighting and displaying.

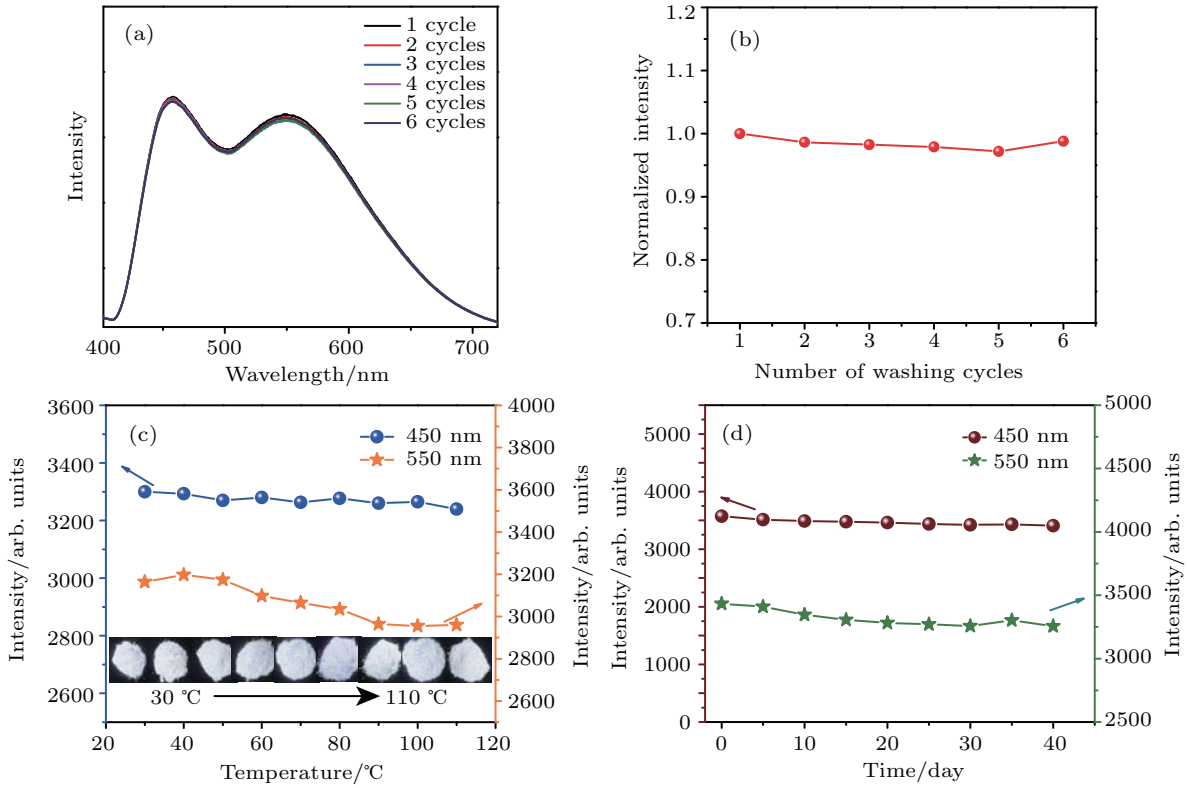


Fig. 6. (color online) (a) The fluorescence intensity of the ZSPN nanocomposite after washing for 6 cycles; (b) the structural stability of the ZSPN nanocomposite; (c) the fluorescence intensity of the ZSPN nanocomposite after annealing; (d) the temporal stability of the ZSPN nanocomposite.

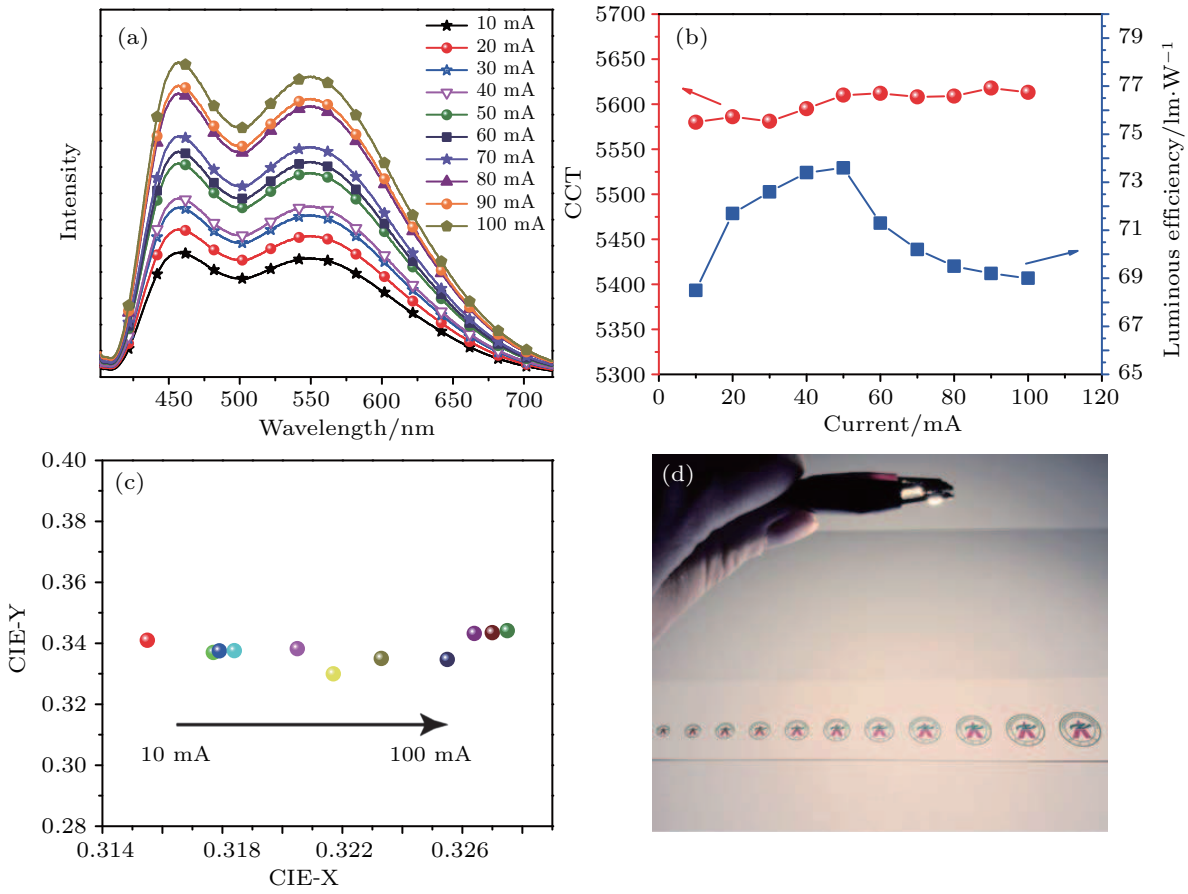


Fig. 7. (color online) (a) EL spectra of the WLED coated with the ZSPN phosphors under different driven currents from 10 mA to 100 mA; (b) CCT and luminous efficiency of the fabricated LED under different driven currents; (c) CIE of the fabricated LED under different driven currents; (d) the photochrome image taken under the illumination of the WLED.

Table 1. Summary of the luminous efficiency for recent reported quantum dots based phosphors

Material	Luminous efficiency	Peaks	Reference	Year
Carbon Quantum Dots	31.3 lm/W	450/525/615 nm	11	2017
$CuInS_2$-based nanocrystals	70 lm/W	550 nm	35	2013
single-phase CdS quantum dots	0.233 lm/W	575 nm	36	2018
Carbon-Nanodots@$BaSO_4$	21 lm/W	540 nm	8	2017
Carbon-ZnO Alternating Quantum Dot Chains	20.1 lm/W	550 nm	37	2018
ZnO-Silica-Phosphors core–shell nanocomposite	73.6 lm/W	550 nm	This work	–

4. Conclusion and perspectives

In conclusion, the efficient and stable ZSPN phosphors have been prepared via a sol-gel synthesis process. The efficient white emission has been achieved from the ZSPN nanocomposite due combine yellow emission from the ZnO QDs with blue emission from the $BaMgAl_{10}O_{17}:Eu^{2+}$ and the PLQY of the ZSPN can reach 63.7%. In addition, the fluorescence intensity of ZSPN nanocomposite shows little decrease even the ambient temperature up to 110 °C or stores in ambient environment for 40 days, indicating the good thermal stability and temporal stability of the ZSPN nanocomposite. The ZSPN nanocomposite has been applied as white emission conversion layer and has been coated onto the UV chips to fabricate WLED. The CCT, CIE, luminous efficiency and CRI of the LEDs are 5580 K, (0.32, 0.34), 73.6 lm/W and 87, which is close to the standard values of warm white emission. Thanks to the low-cost and eco-friendly characters of ZnO, the results reported in this paper may provide a promising pathway towards healthy WLEDs.

References

[1] Wang Z J, Yang Z P, Guo Q L, Li P L and Fu G S 2009 *Chin. Phys. B* **18** 2068
[2] Lee S, Chan T and Chen T 2014 *Acs Appl. Mater. Inter.* **7** 40
[3] Lv W, Jia Y, Zhao Q, Jiao M, Shao B, Lü W and You H 2014 *Adv. Opt. Mater.* **2** 183
[4] Wen Y, Sheng T, Zhu X, Zhuo C, Su S, Li H, Hu S, Zhu Q and Wu X 2017 *Adv. Mater.* 1700778
[5] Sun C, Zhang Y, Sun K, Reckmeier C, Zhang T, Zhang X, Zhao J, Wu C, Yu W W and Rogach A L 2015 *Nanoscale* **7** 12045
[6] Sher C W, Lin C H, Lin H Y, Lin C C, Huang C H, Chen K J, Li J R, Wang K Y, Tu H H, Fu C C and Kuo H C 2016 *Nanoscale* **8** 1117
[7] Zhai Y, Zhou D, Jing P, Li D, Zeng H and Qu S 2017 *J. Colloid. Interf. Sci.* **497** 165
[8] Zhou D, Zhai Y, Qu S, Li D, Jing P, Ji, Shen D and Rogach A L 2017 *Small* **13** 1602055
[9] Sun M, Qu S, Hao Z, Ji W, Jing P, Zhang H, Zhang L, Zhao J and Shen D 2014 *Nanoscale* **6** 13076
[10] Chen Y, Zheng M, Xiao Y, Dong H, Zhang H, Zhuang J, Hu H, Lei B and Liu Y 2016 *Adv. Mater.* **28** 312
[11] Wang Z, Yuan F, Li X, Li Y, Zhong H, Fan L and Yang S 2017 *Adv. Mate* **29** 1702910
[12] Hussain S K and Yu J S 2017 *RSC Adv.* **7** 13281
[13] Bandi V R, Grandhe B K, Woo H, Jang K, Shin D, Yi S and Jeong J 2012 *J. Alloy Compd.* **538** 85
[14] Li X, Budai J D, Liu F, Howe J Y, Zhang J, Wang X, Gu Z, Sun C, Meltzer R S and Pan Z 2013 *Light: Sci. Appl.* **2** e50
[15] Zeng J H, Su J, Li Z H, Yan R X and Li Y D 2005 *Adv. Mater.* **17** 2119
[16] Hirosaki N, Xie R J, Kimoto K and Sekiguchi T 2005 *Appl. Phys. Lett.* **86** 211905
[17] Guo H, Wang Y, Li G, Liu J, Feng P and Liu D 2017 *J. Mater. Chem. C* **5** 2844
[18] Zhu Z, Fu G, Yang Y, Yang Z and Li P 2017 *J. Lumin* **184** 96
[19] Cui H, Zhu P, Zhu H, Li H and Cui Q 2014 *Chin. Phys. B* **23** 057801
[20] Pradal N, Potdevin A, Chadeyron G, Bonville P, Caillier B and Mahiou R 2017 *Opt. Mater.* **64**
[21] Zhu L, Xu L, Wang J, Yang S, Wang C F, Chen L and Chen S 2012 *RSC Adv.* **2** 9005
[22] Wang R, Wei X, Qin L, Luo Z, Liang C and Tan G 2017 *Nanoscale Res. Lett.* **12** 59
[23] Kim H H, Park J S, Han I K, Ok W S, Park C, Hwang D K and Choi W K 2016 *Nanoscale* **8** 19737
[24] Guo X, Wang C F, Yu Z Y, Chen L and Chen S 2012 *Chem. Commun.* **48** 2692
[25] Chen J, Liu W, Mao L H, Yin Y J, Wang C F and Chen S 2014 *J. Mater. Sci.* **49** 7391
[26] Zhang F, Feng X, Zhang Y, Yan L, Yang Y and Liu X 2016 *Nanoscale* **8** 8618
[27] Wang Y, Wang K, Han Z, Yin Z, Zhou C, Du F, Zhou S, Chen P and Xie Z 2017 *J. Mater. Chem. C* **5**
[28] Zhao B, Yao Y, Yang K, Rong P, Huang P, Sun K, An X, Li Z, Chen X and Li W 2014 *Nanoscale* **6** 12345
[29] Xiong H 2013 *Adv. Mater.* **25** 5329
[30] Liu K K, Shan C X, He G H, Wang R Q, Sun Z P, Liu Q, Dong L and Shen D Z 2017 *J. Mater. Chem. C* **5**
[31] Guo D, Shan C, Qu S and Shen D 2014 *Sci. Rep-UK* **4** 7469
[32] Jin Z, Gao L, Zhou Q and Wang J 2014 *Sci. Rep-UK* **4**
[33] Gedamu D, Paulowicz I, Kaps S, Lupan O, Wille S, Haidarschin G, Mishra Y K and Adelung R 2014 *Adv. Mater.* **26** 1541
[34] Liu K, Shan C, Zhou R, Zhao Q and Shen D 2017 *Opt. Mater. Expres* **7** 2682
[35] Chen B, Zhong H, Wang M, Liu R and Zou B 2013 *Nanoscale* **5** 3514
[36] Sun C, Zhang Y, Ruan C, Yin C, Wang X, Wang Y and Yu W W 2016 *Adv. Mater.* **28** 10088
[37] Liu K K, Li X M, Cheng S B, Zhou R, Liang Y C, Dong L, Shan C X, Zeng H B and Shen D Z 2018 *Nanoscale* **10** 7155